PARAMETRIC STUDY OF SWEETENING PROCESS OF SOUR GAS BY MOLYBDENUM OXIDE NANOPARTICLES

Amir Hosseini[1] and M. Nabipoor Hassankiadeh[1,*]

[1]Production Department, Phases 9&10, South Pars Gas Complex (SPGC), National Iranian Gas Company, Assaluyeh, Iran
*Corresponding author: Mojtaba Nabipoor Hassankiadeh, South Pars Gas Complex, Phases 9&10, Assaluyeh, Iran,
P.O.Box:85391-311; Tel. :(+987731)317364; Fax: (+987731)317740; Email: mojtabanp@yahoo.com

Abstract – The purpose of this work is to study the application of nano-molybdenum oxide adsorbent in gas sweetening process. Experiments were made to evaluate the operating and geometrical parameters in the adsorption process. The process performance of H_2S removal from methane gas on molybdenum oxide nanoparticles was defined as the ratio of final concentration of H_2S on the initial concentration of H_2S. The effects of operating conditions such as operating temperature, pressure, the size of nanoparticles, the amount of H_2S concentration in feed stream, feed superficial velocity, and the bed length were studied in this paper. Different temperature values (65, 75, 85, 87 and 89 °C) and pressure values (10, 13, 16 and 19 bar) were applied on the adsorption bed with 19 cm length and 10 cm diameter. Two types of spherical and cylindrical nanoparticles were applied and the effect of different adsorbents diameters (54, 58, 73, 77 and 83 nm) on the process quality (C/C_0) was investigated. Also, the effect of initial concentration of H_2S in the feed gas stream was surveyed. The optimum operating conditions for spherical and cylindrical types were the same, 16 bar and 85 °C. The adsorption capacity of 0.22 g H_2S/g MoO_2 and 0.19 g H_2S/g MoO_2 was achieved at the optimum conditions using nano-spherical and nano-cylindrical MoO_2 sorbent, respectively. Applying in our study two adsorption isotherms, the Langmuir and Freundlich isotherms, analysis of variance displayed a high coefficient of determination (R^2) value of 0.989 for the Freundlich isotherm, indicating the satisfactory adjustment of the experimental data. The results can be interesting for related industries and can be applicable in process optimization.

Keywords: Parametric study, Sweetening process, Molybdenum oxide, Nanoparticle Adsorbent, adsorption isotherm.

INTRODUCTION

The natural gas (NG) extracted from independent gas wells usually contains a large percentage of methane gas, some quantity of ethane and a little quantity of other alkanes and small amount of impurities such as carbon dioxide (CO_2), nitrogen, hydrogen sulfide (H_2S) etc. (Mandal et al. 2004; Alie et al. 2005). Among the non-hydrocarbon components existing in NG, CO_2 and H_2S

may inflict severe damages on both the environment and industrial equipments.

Hydrogen sulfide is a familiar impurity in natural gas streams, coal gas and chemical feed stocks (Niu et al. 2012; Rao et al. 2012; Zhang et al. 2013). Sulfur compounds in fuels such as methane gas cause problems in two ways: they release toxic gases during combustion, and they damage metals and catalysts in engines and fuel cells (Hazrati et al. 2014). Because of the fact that it is a

---

* To whom correspondence should be addressed

very hazardous, toxic, corrosive and pyrophoric gas, H_2S removal has been unavoidably studied applying various methods. Methods of sulfur compounds removal from sour gas, sour oil and furnace exhaust gases have been studied for over 150 years. Early ideas for sour gas, oil and flue gas desulfurization were established in England around 1850 (Niu et al. 2012), one of the most well-known of which is absorption. In this process, sulfur compounds are removed using a liquid treatment that absorbs the sulfur from natural gas, but this process is cumbersome and requires that the gas be cooled and reheated (Wu et al. 2003). To solve these problems, researchers have turned to solid metal oxide adsorbents and some studies have found that sulfur adsorption works best at the surface of solid metal oxides (Balouria et al. 2013). Hydrotreaters now occupy a central role in modern refineries and more than 50% of all refinery streams (Topsoe et al. 1996; Habibi et al. 2010). Hydro-desulfurization is the largest application of catalytic technology in terms of the volume of processed material (Ma et al. 1994). Commercial hydrotreating catalysts are, typically, molybdenum and zinc. Molybdenum, known for its high hydrogenation activity, is preferred as a promoter when feed stocks containing high amounts of nitrogen and aromatics need to be processed. Despite the solid metal adsorbents work at higher temperatures and eliminate the necessity to cool and reheat the fuel, they lose their activity after only a few cycles of use (Christoforidis et al. 2012). Therefore, the metal adsorbents performance is limited by stability issues. So, the authors have set out to create a material with maximum surface area. The solution seemed to be tiny grains of metal oxide nanoparticles, uniting high surface area, high reactivity, and structural integrity in a high-performance sulfur compounds adsorbent. Apparently, nanoparticles such as metal oxides can promote the heating and cooling process. The nano-substances can also enhance the thermal stability of some of materials (Novochimskii et al. 2004; Habibi et al. 2009).

In spite of the interesting catalytic properties of molybdenum oxide, a very limited number of studies have been conducted examining the potential of MoO_2 as an adsorbent for sweetening processes (Flores et al. 2010; Ellefson et al. 2012; Katrib et al. 1996). Such studies were carried out using commercial MoO_2, with particle sizes in the range of a few micrometers and BET surface areas <10 m^2/g. Molybdenum oxide (MoO_2) is a transition metal oxide that has long been known to be active for hydrocarbon decomposition and recently has shown high reforming activity for various long-chain hydrocarbons (Ellefson et al. 2012; Katrib et al. 1996). Researchers have shown that MoO_2 is highly active for reforming isooctane via partial oxidation (Ellefson et al. 2012; Katrib et al. 1996).This process is exothermic ($\Delta H° = -659.9$ kJ/mol) and in the presence of MoO_2 proceeds to full conversion at 700 °C and 1 atm. The catalytic activity shown by MoO_2 can be explained in terms of the Marsvan Krevelen mechanism,

which involves the consumption of nucleophilic oxygen ions provided by the oxygen sub-lattice with the purpose of sustaining the redox cycles taking place on the adsorbent surface. By utilizing nanoparticles, it has been shown that it is possible to significantly increase the total reactive surface area and thus achieve reforming processes with much higher efficiency levels than those of commercial MoO_2. Under similar environments, commercial low surface-area MoO_2 quickly deactivates due to coke formation and sulfur poisoning (Flores et al. 2010). This work is devoted to using experimental design methodology to identify the effect of distinct morphologies of spherical and cylindrical nano-MoO_2 on H_2S adsorption from a gas stream. The adsorption process variables such as temperature, pressure, nanoparticle sizes, space velocity and H_2S feed concentration are also evaluated. The adjustable parameters of Langmuir and Freundlich isotherms are obtained from regression of experimental data and model prediction. The results can be interesting for related industries and can be applicable in process optimization as well as a feasibility point of view.

MATERIALS AND METHOD

Figure 1 shows the gas sweetening experimental set up. One laboratory cylindrical vessel equipped with a nano-molybdenum oxide fixed bed (10 cm diameter and 19 cm length) was applied for the H_2S adsorption process. All equipment's were made of stainless steel since it is a less-corrosive material. A sour methane feed tank containing H_2S and methane gas was used and the flow rate was adjusted by two valves. After passing a filter and an electrical heater, the sour gas stream passed through a compressor. The process temperature was adjusted by the electrical heater and an adiabatic protection surrounded the reactor to keep the bed at the experimental temperature, steadily. The gas was compressed and passed through a filter again and then was fed into the reactor with an adjusted flow rate.

MoO_2 Nanoparticles were synthesized by reduction of molybdenum trioxide (MoO_3) powder in a 1:3 volume ratio of ethylene glycol to distilled water (Flores et al. 2010). The mixture was combined in a 45 ml Teflon-lined general-purpose vessel, which was subsequently sealed and heated to 180 °C for 12 h. After cooling, the dark colored MoO_2 was filtered and air dried at 100 °C. Changing the operating conditions in the synthesis of molybdenum oxide caused different structures of this metal oxide.

The method for production of amorphous spherical and cylindrical MoO_2 nanoparticles is using ultrasonic radiation at ambient temperature and pressure by an ultrasonic vacuum chamber during synthesis. In sonication synthesis, the size and shape of nanoparticles can be controlled without affecting the properties of the material. Nanostructured molybdenum particles prepared in this way,
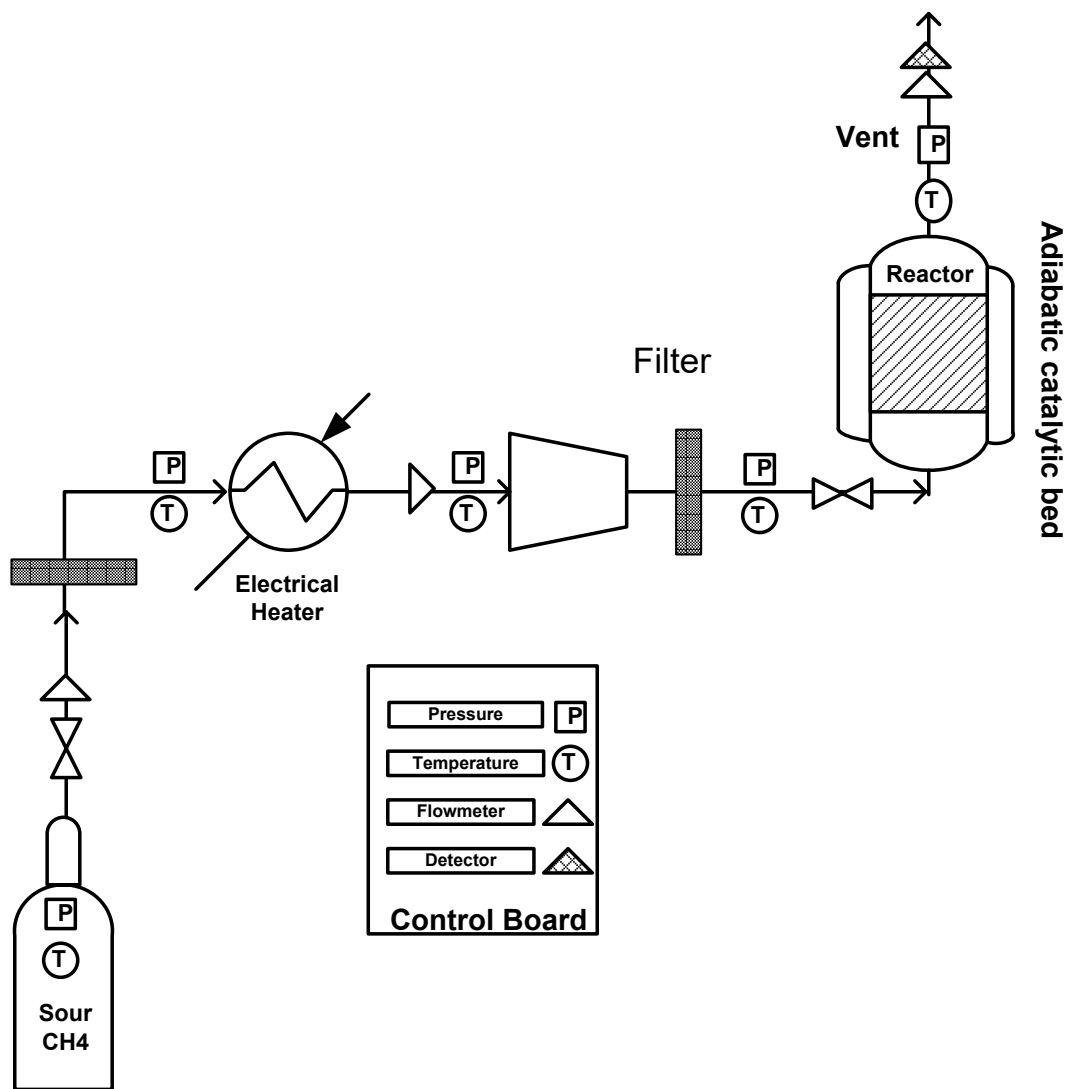
Figure 1. Schematic diagram of the experimental set up.

formed grain sizes which were easily discernable by XRD upon drying. The simplest and most widely used method for estimating the average nano-size particles is using the Scherrer equation (Kaeble, 1967). Using ultrasonic vacuum photoelectron spectroscopy with low energy ion scattering 400-600 watt and 20-30 min exposure time to the ultrasound, spherical nanoparticles were generated. While, when the exposure time was between 30-40 min, cylindrical nanoparticles were produced.

The crystal structure studies of the solids were carried out by a Rigaku Geigerflex x-ray diffractometer using a Cu K_α (λ=1.5418 Å) radiation source with a nickel filter. Also the particle size and morphology of the particle samples were examined using both SEM (FEI Sirion operated at 15 kV) and TEM (Philips CM-200 kV). BET surface area measurements were performed using a multipoint micrometrics 2100E machine.

RESULTS AND DISCUSSION

In this study, experiments are held to evaluate the effect of process operating and geometrical conditions of the nanoparticles and also nanoparticle diameter on the process performance. The ratio of the H_2S final concentration to the initial concentration of H_2S is considered as the criteria of the performance quality of the sweetening process. Experimental results are presented in this section and the optimum conditions which lead to the higher performance quality can be surveyed by analyzing the experimental data.

Adsorbent characterization

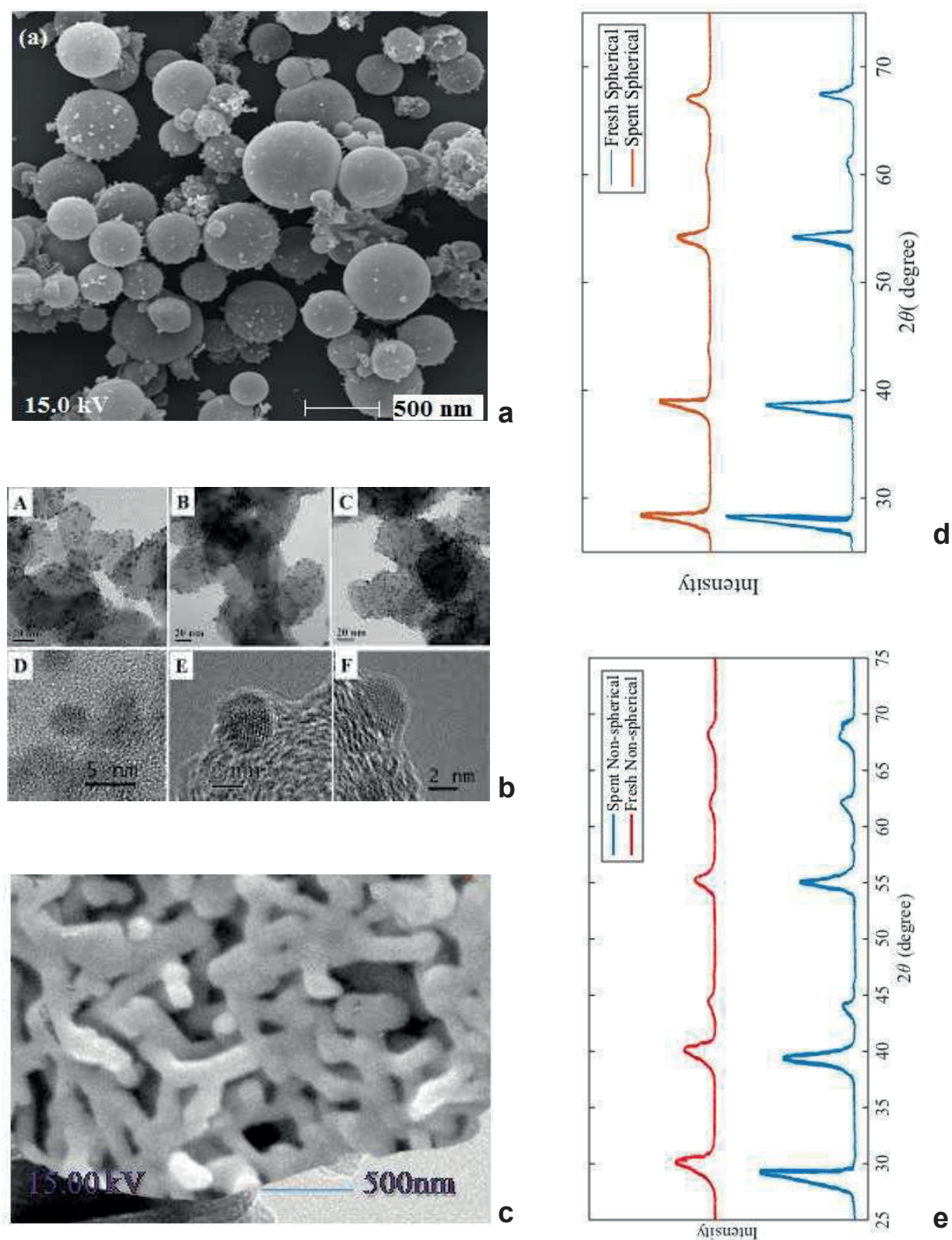Figures 2(a-b) and 2(c) show scanning electron microscope (SEM) and transmission electron microscope

Figure 2. (a) The SEM image of synthesized spherical molybdenum oxide nano particles; **(b)** cylindrical molybdenum oxide; **(c)** The TEM images of molybdenum oxide nanoparticles (A, B and C) cylindrical type. D, E and F spherical type molybdenum oxide nanoparticles; **(d)** XRD patterns of nano molybdenum catalysts before and after H_2S adsorption (line a) spherical like fresh nano-MoO_2, (line b) spherical like nano-MoO_2 after sweetening process; **(e)** XRD patterns of nano molybdenum catalysts before and after H_2S adsorption (line c) cylindrical like fresh nano-MoO_2, (line d) cylindrical like nano-MoO_2 after adsorption.

(TEM) images of nanoparticle MoO_2, respectively. These images indicate that the agglomerates consist of nanoparticle MoO_2 produced with the average diameter of 54-83 nm. By utilizing nanoparticles it is possible to significantly increase the total surface area, a much more uniform particle size and shape, consisting of equiaxial particles with average size of about 20nm. Figures 2(d) and 2(e) depict the XRD of synthesized molybdenum oxide nanoparticles. These Figures show X-ray diffraction patterns obtained from both the spherical and cylindrical MoO_2. In both cases, only the peaks for the distorted rutile structure of the MoO_2 phase are present. The most intense peak for the nano-spherical MoO_2 and nano-cylindrical MoO_2 is at $2\theta = 35°$ and $2\theta = 38°$, respectively. It is well worth noting that, there are important differences among the diffraction patterns of spherical and cylindrical nanoparticles as shown in Figures 2(d) and 2(e). Figure 2(d) shows that nano-MoO_2 sorbent with spherical morphology could remove H_2S better than nano-cylindrical MoO_2 and it can be indexed exclusively to MoS_2 (this was confirmed by XRD, which showed different peaks for MoS_2 in spherical type). Moreover, it can be seen from these Figures that the intensity of MoO_2 peaks after H_2S adsorption decreased while a combination of metal oxides and metal sulfides is formed. These results verify that some crystalline structural changes have occurred after H_2S adsorption.

The effect of operating temperature and pressure

Both, temperature and pressure are two important parameters in separation processes. The changes in the operating pressure and temperature on the performance quality are illustrated in Figures 3 and 4. The feed stream contains 58 ppm of H_2S. Operating pressure were changed in values of 10, 13, 16 and 19 bar and operating temperature were varied in values of 65, 75, 85, 87 and 89 °C considering to the usual conditions in the adsorption reaction of H_2S, strength of equipment and safety regulations in the laboratory. Two types of cylindrical and spherical shape nanoparticles with 77 nm in diameter were applied in the adsorption bed. According to Figure 3, the increment in the operating pressure, increased the process quality at 65 and 75 °C and at all pressure values, generally using cylindrical type. However, this trend changed for 13 bar and 89 °C, 16 bar and 85, 87 and 89 °C. As the temperature at the applied pressure increased a reduction in diffusivity of H_2S in the MoO_2 pores and product layer was expected. The observed result is in accordance with the reports given by Navochinskii et al. So, 89 °C and temperatures higher than 85 °C are not proper operating temperatures at 13 bar and 16 bar, respectively. Also, an increase in the pressure value from 13 bar to 16 bar showed the considerable decrease in the value of C/C_0. The higher pressures 16 bar and 19 bar present lower value of C/C_0 at the higher temperature. So, the case of determination of the minimum values of

energy consumption can be discussed here. However, considering the strength of the reactor vessel, the higher temperatures (87, 89 °C) result in a better value of C/C_0 at lower pressures of 10 bar and 13 bar.

Operating conditions of 16 bar and 85 °C can be introduced as the optimum operating conditions in the experiments. This is determined due to the marketing standard value of H_2S in the sweet gas stream which is lower than 4 ppm, i.e., 3.54 ppm at 16 bar and 85 °C.

Figure 4 shows the changes in the values of C/C_0 according to the changes in the operating temperature and pressure using spherical nano-MoO_2. The lower values of C/C_0 were obtained at higher temperatures and constant pressure. The increase in the pressure value from 13 bar to 16 bar decreased the value of C/C_0 considerably, comparing with the changes from 10 to 13 bar or 16 to 19 bar. The higher pressure values resulted in lower values of C/C_0 using 75 and 85 °C; however, this was not obtained at temperatures higher than 85 °C initializing the operating pressure of 16 bar and 19 bar. This might be related to the effective operating pressure of the gas stream in the nanoparticle bed, which provides the proper effective gas diffusion into the adsorbent at the adjusted temperature.

The effect of nanoparticle diameter

In this section, nano-molybdenum oxide adsorbents with five different diameters are applied in separate experiments. The changes in the diameter of nanoparticles affect the value of C/C_0 as shown in Figures 5 and 6 using spherical and cylindrical nanoparticles, respectively. According to the results which were obtained above, the optimum operating temperature, 85 °C, and pressure 16 bar were considered in the experiments. At the optimum pressure 16 bar and temperature of 85 °C in the adsorbent bed with length of 3 cm and 8 cm diameter included spherical nanoparticle, the changes in the value of C/C_0 were investigated with various particle diameters, 54, 58, 73, 77 and 83 nm. The ratio of the bed diameter on the bed length was relatively large (2.67) and assumed to provide proper distribution and reaction surface area, avoiding channeling. However, changes in particle diameter showed considerable effect on the value of C/C_0 for both spherical and cylindrical nanoparticles, even in this provided bed.

While it appears to be an oscillatory trend, Figures 5 and 6 show that there is a higher value of C/C_0 using larger nanoparticles in diameter on the whole. This might be related to the larger effective surface area provided by the smaller nanoparticles in the specified geometry of the bed. The smaller particles also form a thinner gas boundary layer around the particles, which is responsible for convective mass transfer in the gas phase. Smaller particles make diffusion mass transfer faster and so molybdenum oxide with smaller nanoparticles improves the adsorption capacity, which must be the result of more surface area.
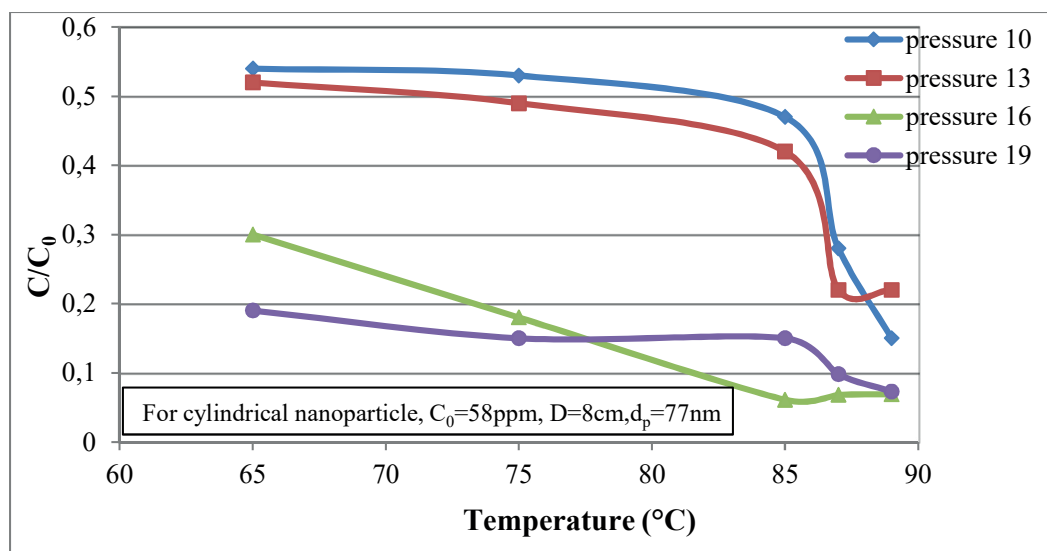
Figure 3. Performance quality versus operating conditions using cylindrical nano adsorbent
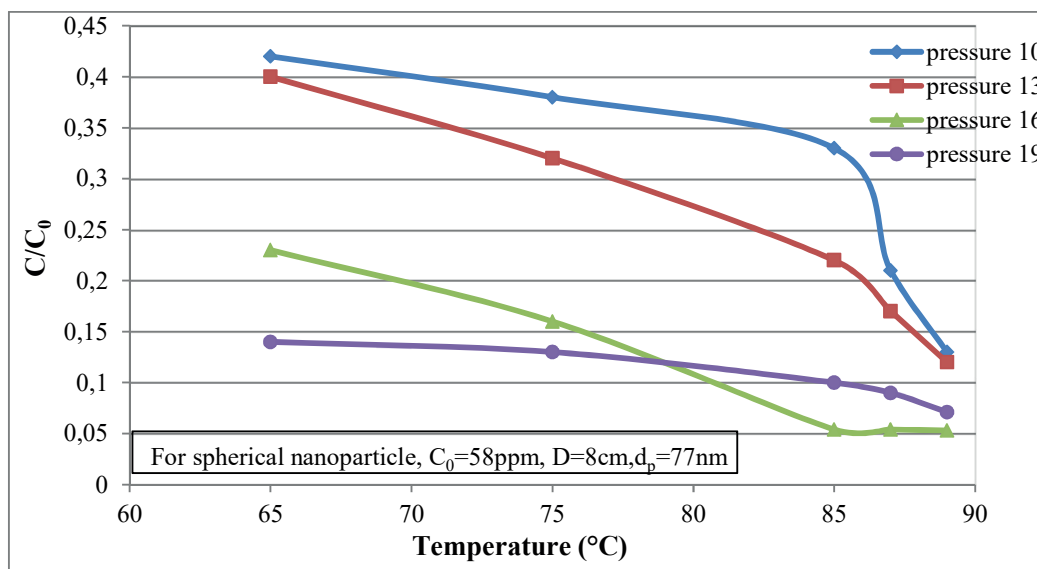

Figure 4. Performance quality versus operating conditions using nano-spherical adsorbent

Considering the most important part of our study, which was studying the influence of sorbent morphology on H_2S adsorption, the morphology of spherical and cylindrical sorbents was characterized using the dynamic capacity of H_2S removal (C/C_0). Comparing the results from Figure 5 and Figure 6 shows that the spherical and cylindrical type of nanoparticle 58 nm in diameter had the lowest value of C/C_0 of about 0.032 and 0.044, respectively. This may relate to the proper arrangement of spherical geometry compared with the cylindrical geometry in the defined dimensions of adsorbent bed. It is noticeable that the range of dynamic H_2S adsorption capacity of MoO_2 was 0.025-0.22 g H_2S/g

MoO_2. Besides, the BET results indicated that the surface areas of cylindrical and spherical nano-MoO_2 were 10 and 48 m^2/g, respectively, which were about an order of magnitude greater than that of the commercially available material (Flores et al. 2010). High surface area was also beneficial for adsorbents as more active sites per volume allow for greater adsorbed flow rates and more efficient adsorption. This result is consistent with the observation given in Sekhavatjou et al. (2014) that, with reduction of iron oxide particle size (from 0.14 μm to 20 nm), the sulfur removal rate increased from 37.9 to 63.1% in all of the natural gas components.
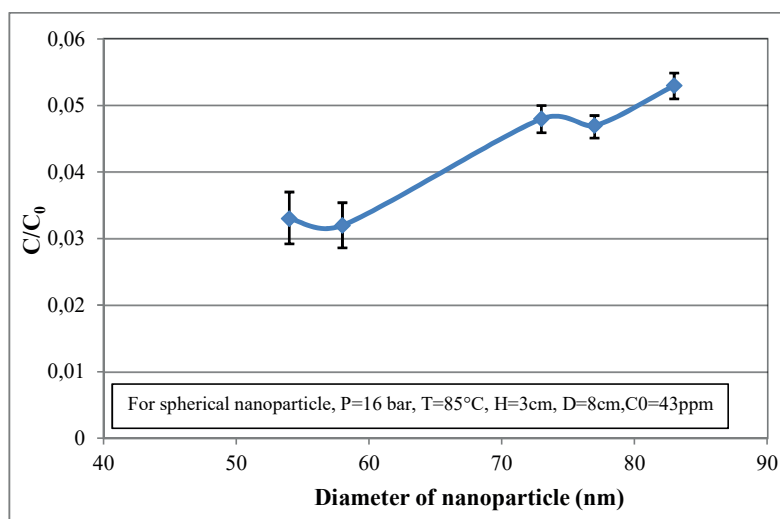
Figure 5. Performance quality versus particle diameter for spherical adsorbent
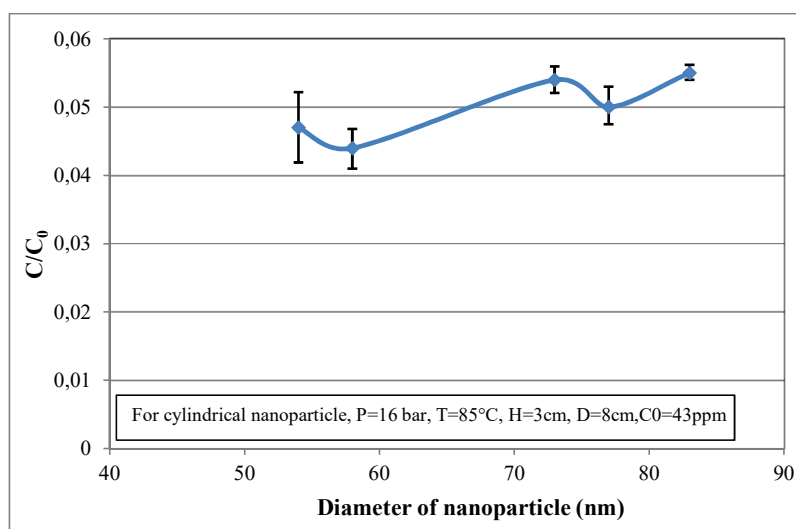

Figure 6. Performance quality versus particle diameter for cylindrical adsorbent.

The effect of initial concentration

The initial concentration of H_2S contaminant in the feed stream provided the driving force for the adsorption reaction. Applying optimum operating conditions of 16 bar and 85 °C for cylindrical and spherical type nano-molybdenum oxide and optimum diameter of 58 nm for both spherical and cylindrical type, the effect of driving force on the adsorption reaction is investigated in Figures 7 and 8.

In each run, a feed stream containing a different concentration of H_2S (38, 43, 58, 64 and 73 ppm) was passed through the bed and the performance quality of the adsorption process was investigated. The performance of the spherical type of nanoparticle did not show any considerable changes using different initial concentrations from 38 ppm to 64 ppm and all the obtained values were in the range of 0.041 to 0.049 ppm. However, the 73 ppm H_2S concentration showed a sudden increase in the value of C/C_0. So, it can be concluded that, for the spherical type of nanoparticle, the effect of initial driving force in the feed stream is not considerable until the concentration of H_2S of 73 ppm in the feed stream.

Figure 8 shows the considerable effect of initial driving force on the value of the adsorption capacity using cylindrical nanoparticle. The changes in H_2S content in the feed gas from 38 ppm to 73 ppm gave values of 0.047 to 0.071 for the value of C/C_0. This indicates that the capacity of nanoparticles is fixed and the active surface site reduction provides a more reasonable explanation for this behavior. So the quality of the adsorption process of H_2S on cylindrical adsorbent is sensitive to the initial concentration of contaminant in comparison with the spherical type.
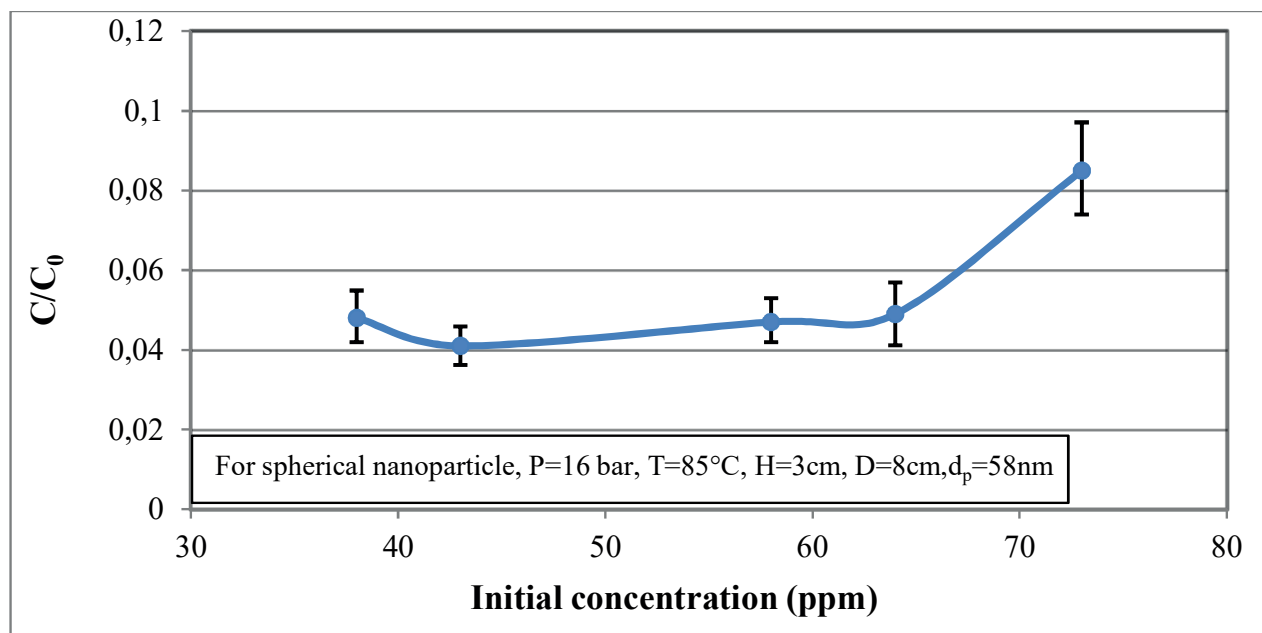
Figure 7. Performance quality versus initial concenration for spherical type
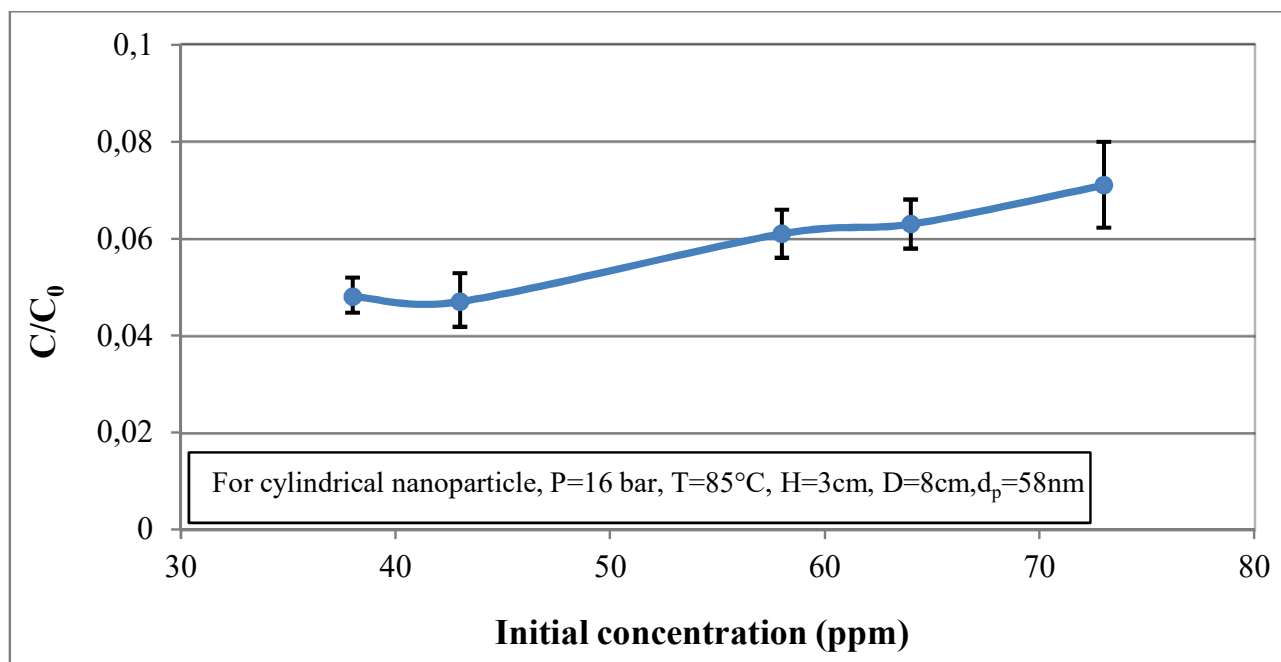

Figure 8. Performance quality versus initial concenration for cylindrical type

The effect of feed superficial velocity

To determine the effect of feed superficial velocity, this parameter was studied in the range of 0.018-0.045 m/s. As is expected, the higher the superficial velocity the less the dynamic H_2S adsorption capacity will be. Lower superficial velocity values provided more time for H_2S component to reach the surface of fresh MoO_2 uncovered with MoS_2. Figure 9 shows that, with the rise in superficial velocity, a higher content of input H_2S emerges from the bed and the value of C/C_0 increases for both spherical and cylindrical nanoparticles. The results were obtained in the aforementioned optimum conditions for spherical and cylindrical nanoparticles.

The effect of bed length

The length of the adsorption bed was changed between 4 cm and 7 cm. The optimum length of the nano-sorbent bed was studied in this section. According to Figure 10, the increment in the bed length improves the H_2S removal for both cylindrical and spherical nanoparticles. However, a slight decrease in the value of C/C_0 was obtained at a length more than 6 cm. So using extra adsorption bed longer than 6 cm did not have a considerable effect on H_2S removal.

Equilibrium mechanism of adsorption

Two adsorption isotherms, Langmuir and Freundlich isotherms are proposed to fit the experimental data. Table 1 demonstrates the isotherms equations used in our study. As can be seen from Figures 11 and 12, the values of the coefficients of determination (R^2) for spherical nanoparticles are 0.969 and 0.989 for Langmuir and Freundlich isotherms, respectively. Being close to 1, the value of R^2 for the Freundlich isotherm ensures the
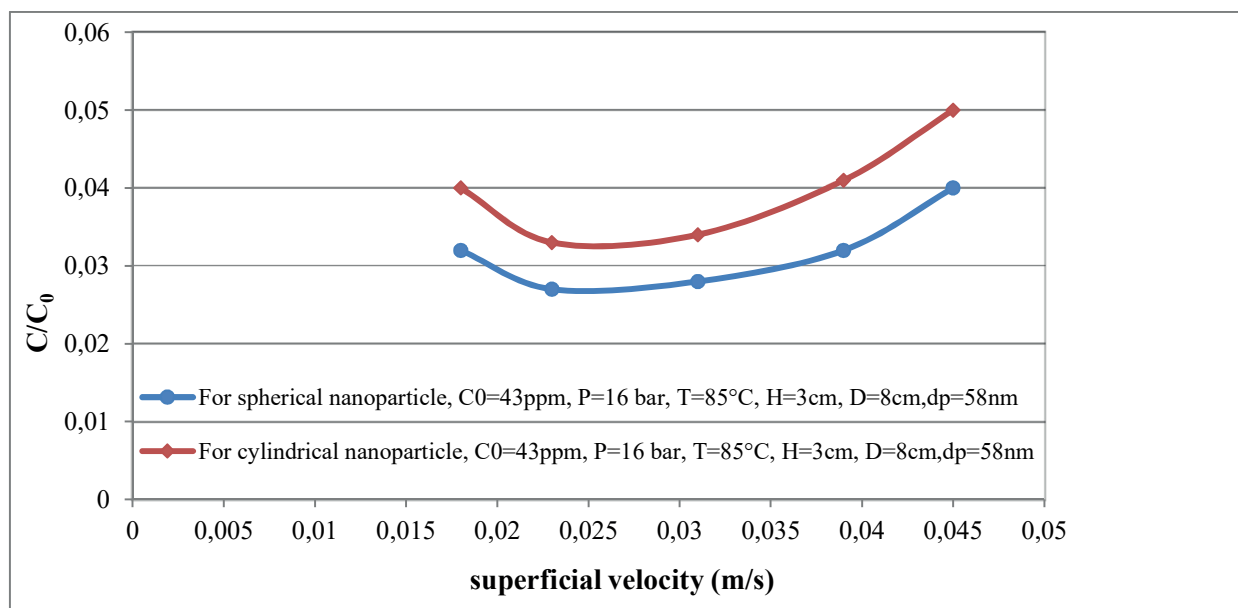

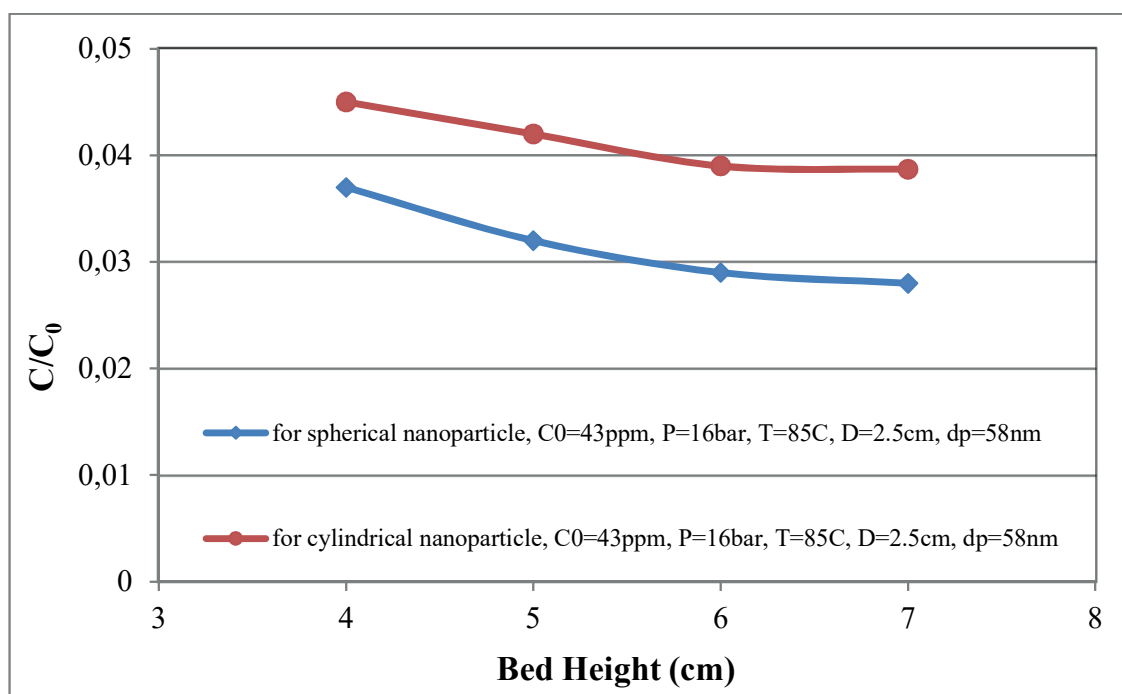**Figure 9.** Performance quality versus feed superficial velocity

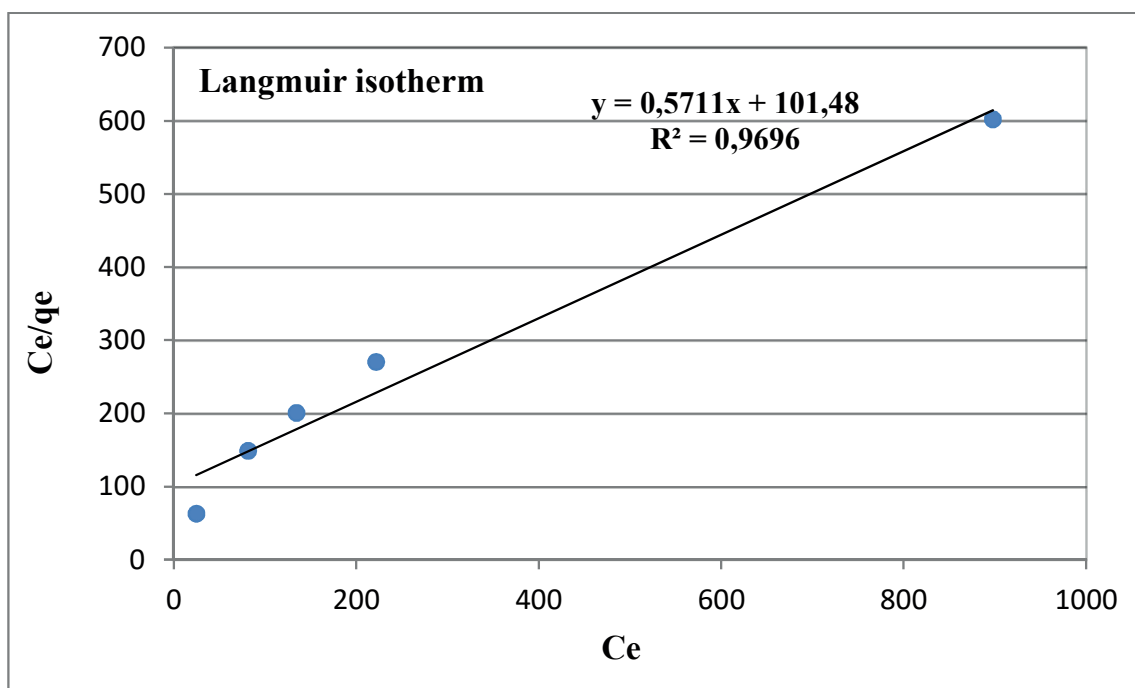**Figure 10.** Performance quality versus molybdenum oxide bed height

Langmuir isotherm

$y = 0{,}5711x + 101{,}48$

$R^2 = 0{,}9696$

Figure 11. Correlation the experimental data with a Langmuir isotherm for spherical nanoparticles

Freundlich isotherm

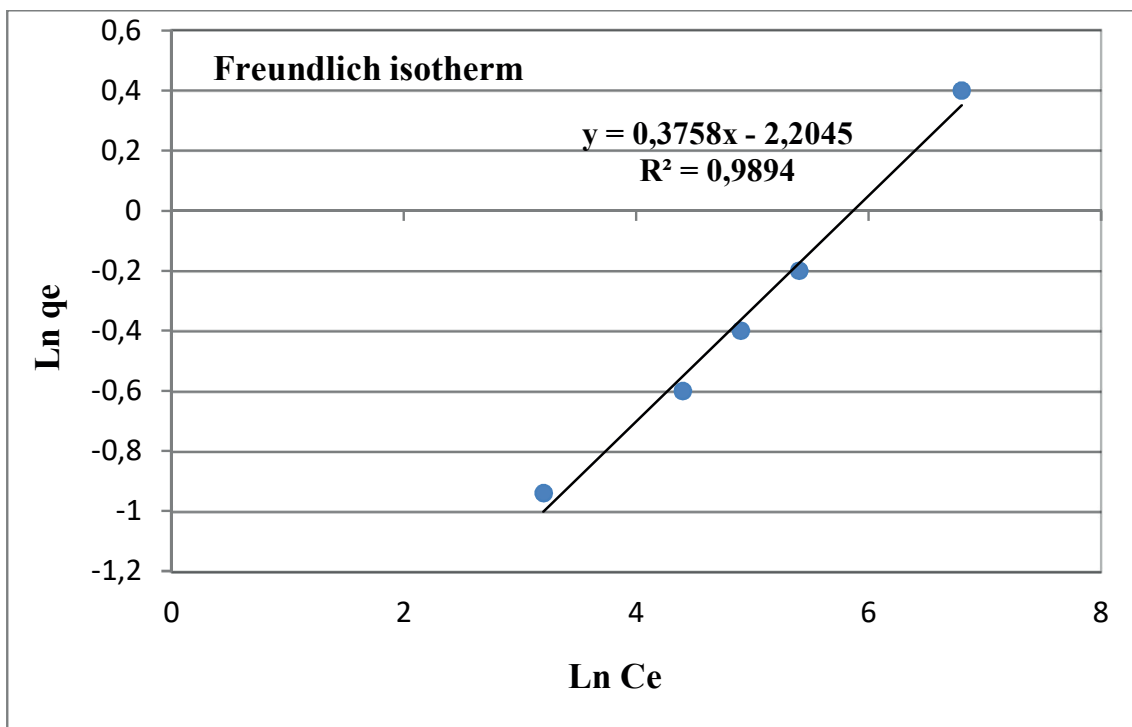$y = 0{,}3758x - 2{,}2045$

$R^2 = 0{,}9894$

Figure 12. Correlation the experimental data with a Freundlich isotherm for spherical nanoparticles

perfectness of the correlation between the predicted and observed values. Thus, the Freundlich isotherm can predict the adsorption of gases by the solid adsorbent more accurately than the Langmuir isotherm. The deficiency of the Langmuir isotherm is that it considers the equilibrium mechanism of adsorption and desorption of reactants and products uniformly across the adsorbent surface and at high pressures the reaction rate is independent of gas

pressure and the surface coverage fraction would be unity. This is consistent with results in the literature (Nabipoor Hassankiadeh and Haghtalab, 2013). The above-mentioned adsorption parameters based on the experimental data are presented in Table 2 for both isotherms.

Table 1. Adsorption isotherms of spherical nanoparticles

	Langmuir isotherm	Freundlich isotherm
	$$\dfrac{c_e}{q_e} = \dfrac{c_e}{q_m} + \dfrac{1}{k_l q_m}$$	$$Ln\, q_e = Ln\, k_f + \dfrac{1}{n}(Ln\, C_e)$$
R^2	0.969	0.989

Table 2. Adsorption parameters of the isotherms

	Langmuir isotherm		Freundlich isotherm	
Parameter	Value	Unit	Value	Unit
k_f	–	–	9.06	L mg^{-1}
n	–	–	2.67	–
k_l	0.006	L mg^{-1}	–	–
q_m	1.75	mg g^{-1}	–	–
β	–	–	–	–

CONCLUSION

The performance quality of a gas sweetening process is surveyed in this study. The effect of parameters which are responsible for mass transfer phenomena such as dimensions of adsorbents, shape of nanoparticles and initial driving force are investigated. In addition, the effect of temperature and pressure on the process quality is considered in this work. The main experimental results are presented as follows:

1. The optimum pressure and temperature for both spherical and cylindrical particles are 16 bar and 85 °C. However, the value of C/C_0 in this optimum condition for the spherical type is 0.054, lower than that obtained (0.061) using the cylindrical type with the same diameter of 77 nm.

2. The optimum value of the adsorbent diameter for the spherical and cylindrical types is 58 nm, which gives the values of 0.032 and 0.044 for C/C_0, respectively.

3. At the optimum operational and dimensional conditions for cylindrical and spherical adsorbents, the initial driving force is not the process controller for the adsorption with the spherical type when the initial concentration of H_2S is lower than 64 ppm. However, changes in the initial concentration of H_2S show gradual and steady changes in the value of C/C_0 from 0.047 to 0.071 when using the cylindrical type of nanoparticle.

4. The capability of nano-molybdenum oxide adsorbents decreases with an increase in the superficial velocity. Moreover, the optimum bed length is 6 cm for both cylindrical and spherical nanoparticles, because the value of C/C_0 decreases slightly at a length larger than 6 cm.

5. Finally, it can be concluded that the Freundlich isotherm is in better agreement with the experimental data than the Langmuir isotherm. Thus, it is possible to predict the H_2S removal capacity relying on the Freundlich isotherm.

REFERENCES

Alie, C., Backham, L., Croiset, E., Douglas, P.L., Simulation of CO_2 capture using MEA scrubbing: a flow sheet decomposition method, Energy Convers. Manage. 46, 475-487 (2005).

Balouria, V., Kumar, A., Samanta, S., Singh, A., Debnath, A.K, Mahajan, A., Bedi, R.K., Aswal, D.K., Gupta, S.K., Nanocrystalline Fe_2O_3 thin films for ppm level detection of H_2S, Sens. Actuators B. 181, 471-478 (2013).

Christoforidis, K.C., Figueroa, S.J.A., Fernández-García, M., Iron-Sulfur Codoped TiO_2 Anatase Nano-Materials: UV and Sun-light Activity for Toluene Degradation, Appl. Catal. B. 18, 310-316 (2012).

Ellefson, C., Flores, O.M., Ha, S., Norton, G., Synthesis and applications of molybdenum (IV) oxide, J. Mater. Sci. 47, 2057-2071 (2012).

Emerson, S.C., Coote, C.F., Boote, H., Tufts, J.C., Larocque, R., Moser, W.R., The ultrasonic synthesis of nanostructured metal oxide catalysts, prep. Catal. 7, 773-785(1998).

Flores, O.M., Turba, T., Ellefson, C., Wang, K., Breit, J., Ahn, J., Nanoparticle molybdenum dioxide: a highly active catalyst for partial oxidation of aviation fuels, Appl. Catal. B. Environ. 98, 186-192 (2010).

Habibi, R., Daryan, J.T., Rashidi, A.M., Shape and size-controlled fabrication of ZnO nanostructures using novel templates, J. Exp. Nanosci. 4, 35-45 (2009).

Habibi, R., Rashidi, A.M., Daryan, J.T., Alizadeh, A.M., A Study of the rod-like and spherical nano-ZnO morphology on H_2S removal from natural gas, Appl. Surf. Sci. 257, 434-439 (2010).

Hazrati, H., Abdouss, M., Vahid, A., Miran Beigi, A.A., Mohammadalizadeh, A., Removal of H_2S from crude oil via stripping followed by adsorption using ZnO/MCM-41 and optimization of parameters, Int. j. Environ. Sci. Technol. 11(4), 997-1006(2014).

Kaeble, E., Handbook of X-Rays, McGraw-Hill, New York, (1967).

Katrib, A., Leflaive, P., Hilaire, L., Maire, G., Molybdenum based catalysts. I. MoO_2 as the active species in the reforming of hydrocarbons, Catal. Lett. 38, 95-99 (1996).

Ma, X., Sakanishi, K., Mochida, I., Hydrodesulfurization reactivities of various sulfur compounds in diesel fuel, Ind. Eng. Chem. Res. 33, 218-222 (1994).

Mandal, B.P., Biswas, A.K., Bandyopadhyay, S.S., Selective absorption of H_2S from gas streams containing H_2S and CO_2 into aqueous solutions of N-methyldiethanolamine and 2-amino-2- methyl-1- propanol, Sep. Purif. Technol. 35, 191-202 (2004).

Nabipoor Hassankiadeh, M., Haghtalab, A., Product Distribution of Fischer Tropsch Synthesis in a Slurry Bubble Column Reactor Based on Langmuir-Freundlich Isotherm, Chem. Eng. Comm. 200 (2013), 1170-1186.

Niu, Y., Xing, M., Tian, B., Zhang, J., Improving the visible light photocatalytic activity of nano-sized titanium oxide via the synergistic effects between sulfur doping and sulfation, Appl. Catal. B. Environ. 5, 253-260 (2012).

Novochimskii, I., Song, C., Ma, X., Liu, X., Shore, L., Lampert, J., Farrauto, R.J., Low temperature H_2S removal from steam containing gas mixtures with ZnO for fuel cell application. 1. ZnO particles and extrudates, Energy Fuels. 18, 576-583 (2004).

Rao, M., Song, X., Cairns, E.J., Nano-carbon/sulfur composite cathode materials with carbon nano-fiber as electrical conductor for advanced secondary lithium/sulfur cells, J. Power Sources, 205, 474-478 (2012).

Sekhavatjou, M.S., Moradi, R., Hosseini Alhashemi, A., Taghinia Hejabi, A., A new method for sulfur components removal from sour gas through application of zinc and iron oxides nanoparticles, Int. J. Environ. Res. 8, 273-278 (2014).

Topsoe, H., Clausen, B.S., Massoth, F.E., Hydrotreating catalysis, Catalysis-Science and Technology, Springer -Verlag, Berlin, p. 1-3 (1996).

Wu, Q., Yakshinskiy, B.V., Madey, T.E., Adsorption and decomposition of H_2S on UO_2 (0 0 1), Surf. Sci. 523, 1-11 (2003).

Zhang, Y., Zhao, Y., Konarov, A., Gosselink, D., Soboleski, H.G., Chen, P., A novel nano-sulfur/polypyrrole/graphene nano-composite cathode with a dual-layered structure for lithium rechargeable batteries, J. Power Sources, 241, 517-521 (2013).